ELSEVIER

Advances in Colloid and Interface Science
61 (1995) 161–189

ADVANCES IN COLLOID AND INTERFACE SCIENCE

The rheology of concentrated suspensions of deformable particles☆

W.J. Frith*, A. Lips

Unilever Research, Colworth Laboratory, Colworth House, Sharnbrook, Bedfordshire MK44 1LQ, UK

Abstract

The rheology of slightly deformable particles, in particular their dilatant behaviour, has been investigated using waxy maize starch as a 'model' suspension. Suspensions of such large particles present considerable experimental problems in rheological terms in that they exhibit phenomena such as wall slip and sedimentation. These are discussed in some detail, along with the methodologies developed to overcome them. Comparisons of the results with hard sphere data in the literature indicate that whilst the deformability of the starch granules does not play a significant role in the high shear limiting viscosity, the dilatant transition does appear to be strongly affected.

Introduction

Dilatancy is a phenomenon seen in many suspensions of relevance to industrial processes, in rheological terms it is manifested as an abrupt rise in suspension viscosity as shear rate is increased, as illustrated in Fig. 1. Because this phenomenon can be extreme in nature (the rise can be as much as 2–3 orders of magnitude) it is generally desirable to avoid

☆ Paper presented at the RSC–CISG Conference on Concentrated Dispersions, Bristol, 29–31 March 1995.

* Corresponding author.

0001-8686/95/$29.00
SSDI 0001-8686(95)00264-2

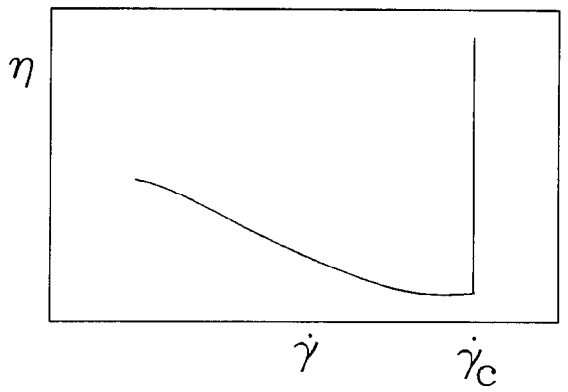

Fig. 1. Illustration of flow curve for a dilatant suspension.

such behaviour. In extreme cases damage to processing plant can occur and in any case the dilatancy places a limit on the rate at which a suspension can be processed, hence understanding and control of this phenomenon is of considerable importance.

Dilatancy is known to have its origins in a structural change occurring in the suspension [1,2], in some cases this is known to be associated with a change from an ordered particle arrangement during normal flow to a disordered structure in dilatant flow [2], whilst in others both structures can be disordered [3]. The origins of the structural change are still poorly understood, though several attempts have been made to model the transition in theoretical terms [4,5] they tend to either rely on particle properties that are not necessarily present in suspensions that display dilatancy or are unrealistic for many classes of suspensions in terms of the microstructural processes proposed (i.e. a Brownian mechanism [5] proposed for sub-micron particles will be invalid for a suspension of 30–100 micron particles which shows dilatancy).

Bearing the above considerations in mind it is still possible to use the proposed mechanisms to make predictions concerning the scaling relationships involved in the dilatant transition. This can be done in terms of its dependence on suspension properties such as particle size, medium viscosity etc. Hence a consideration of the past theoretical work on the subject is of interest.

Mechanisms that have been proposed for the dilatant transition tend to fall into one of two classes, those which involve the Brownian motion of the particles, and those which involve the shear induced hydrodynamic forces on the particles. Early work by Metzner and Whitlock [6]

falls into the former category in that it was suggested that suspensions subjected to high shear-rates formed structures of layered particles, sliding over one another (which was later verified [2], for some systems at least). Movement of particles from one layer to another, supposedly by Brownian diffusion, brings about changes in the momentum of the particles following behind the streamline and leads to disruption of the flow structure, causing shear thickening. A similar mechanism was also discussed by Choi [5] and has the advantage that there is an obvious dimensionless variable that can be employed to characterize the onset of shear thickening. In Choi's [5] discussion it is assumed that particles become trapped between the flowing layers when the shear rate in the suspension becomes comparable to the inverse of the time required for a particle to diffuse its own diameter, as illustrated in Fig. 2. This shear-rate is characterised by the Peclet number ($Pe = \eta_m \dot{\gamma} a^3/kT$) being of order unity, and is thus readily subject to experimental testing. It should be pointed out, however, that the use of the Peclet number is, in principle only valid for dilute suspensions. However, relative effects of changes in the medium viscosity and particle size should be the same irrespective of the concentration, making the use of Pe as a scaling variable valid at high concentrations. The main disadvantage of this type of mechanism is that it is difficult to envisage it being valid for any but sub-micron suspensions, whereas shear thickening is observed frequently in suspensions of much larger particles [7] (>100 μm). Indeed, it may well be that shear thickening can arise through more than one mechanism and that those based on hydrodynamic arguments will only come into play with the larger particles.

Mechanisms involving the hydrodynamic forces on the particles have been proposed by several authors [4,8,9], most notable being the work of Hoffman [2,4]. This work comprised a careful experimental and theoretical study of the flow of suspensions of PVC particles in partially

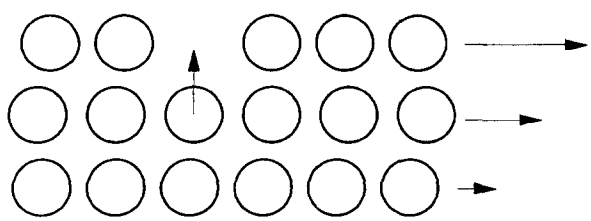

Fig. 2. Particles can diffuse between layers in flowing suspensions but at higher shear rates will become trapped between layers causing dilatancy.

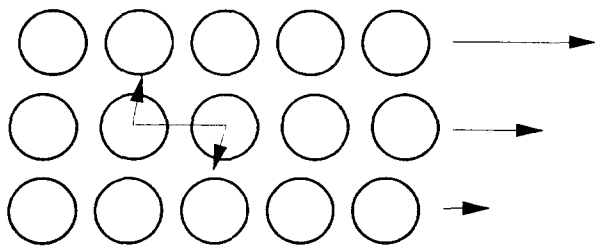

Fig. 3. Shear induced hydrodynamic forces destabilize the flowing layers of particles.

swelling solvents, such as di-butyl phthalate. Rheological measurements were combined with surface diffraction measurements which allowed the observation of the structural changes occurring at the dilatant point. The mechanism proposed by Hoffman assumed that particles within the flowing layers experienced a hydrodynamically induced force that acted to pull them out of their layer and thus disrupt the ordered flow, this is illustrated in Fig. 3. Countering this tendency was a force between the particles, in this case electrostatic, which acted to stabilize the flowing layers. Latterly, this theory has been developed by Boersma [8] for poly(styrene particles). Interestingly this theory highlights the importance, long suspected through general experience, of the role that colloidal forces play in controlling the transition. Unfortunately there is as yet very little systematic evidence of the way in which such forces affect the behaviour of particle suspensions in this flow regime, so little is known for certain. It is, for instance, suspected that long range repulsive forces between particles stabilise the suspension against dilatancy [7,10] but there is still considerable debate as to the effect of attractive forces.

Unfortunately the theories of Hoffman [2] and Boersma [8] require some sort of stabilizing force to counteract the hydrodynamic forces and it is unclear how this might arise in a hard sphere suspension where the only forces are Brownian or hydrodynamic, this reduces the predictive capabilities of such theories for the suspensions used in this study. However, it is still possible to use the model to predict scaling effects such as those due to changes in particle size or medium viscosity. For instance, the transition is expected to be proportional to $1/a^2$ and $1/\eta$, which makes comparison with other theories possible.

An additional problem with the type of theory proposed by Hoffman lies in the basic assumptions involved in calculating the forces on the particles. It is proposed that hydrodynamic forces on pairs of particles

act to rotate them out of the ordered layers of the flowing suspension. However each particle in the suspension will have forces acting upon it from two pairs of particles, as illustrated in Fig. 3 the resultant force on the particle will, averaged over time, be zero. If this is assumed to be the case then there is no mechanism for the destabilization of the particle layers as the shear rate increases.

One assumption common to all the above mechanisms for dilatancy in suspensions is that the phenomenon involves a transition from an ordered, non-dilatant structure to a disordered, dilatant one. On the face of things this is rather surprising since many suspensions that display dilatancy are made up of particles that are either not mono-sized or not spherical or both [7]. In addition, some recent work by Laun [3] and co-workers has shown that even monosized spherical particles are not necessarily ordered prior to shear thickening. These observations cast doubt on the validity of the above mechanisms.

An additional point to note is that recent simulation work by Melrose and co-workers [11], and some classical calculations by Marrucci [12] has shown that hard spheres, under the type of flow conditions encountered here will have minimum surface to surface separations approaching atomic radii. At such separations it is difficult to argue that hard sphere hydrodynamics will have any validity and thus casts more doubt on mechanisms based on the hard sphere model. Despite this it is still interesting to compare the predicted behaviour with that observed in experimental systems in order to gain insight into the origins of the shear thickening phenomenon.

As already mentioned, long range forces between particles are believed to have a profound effect on the dilatant transition. It is known, for instance, that long range repulsive forces between particles will stabilise the suspensions against dilatancy [7,10], this is also true for the case of deformable particles, and one of the main aims of this work is to investigate the effect of particle deformability on the dilatant transition and on the rheology in general.

One problem associated with past studies on dilatant systems is the abrupt nature of the viscosity rise with increasing shear rate (Fig. 1). This makes it very difficult to study the phenomenon using a controlled shear-rate instrument, which was, until recently, the only type of instrument available. When measuring shear thickening similar to that in Fig. 1 on a controlled shear rate instrument the abruptness of the transition will tend to give rise to a disruption of the sample at shear-rates above the dilatant point and possibly lead to damage to the

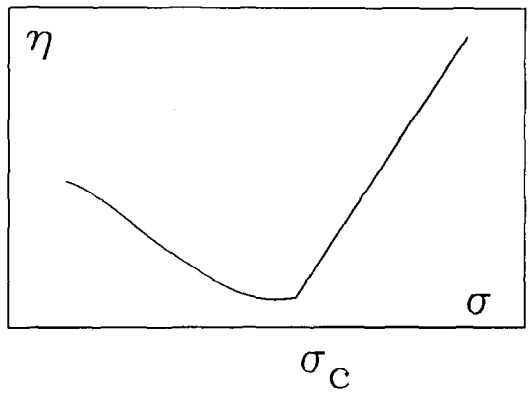

Fig. 4. Illustration of the viscosity shear stress relationship for a dilatant suspension.

rheometer. As a result careful study of dilatancy is more appropriately conducted using a controlled shear stress instrument.

If the curve in Fig. 1 is replotted as viscosity versus shear stress rather than shear rate then the abrupt rise in viscosity is no longer present (Fig. 4), allowing detailed study of the transition region to be made. The use of controlled stress rheometers thus offers considerable advantages, as can be seen from recent work in the area [3,13].

Materials and methods

Materials

Corn starch (waxy maize) was selected as an initial material for study, because its swelling characteristics in water make it a suitable model for deformable particles. Such suspensions have been studied quite extensively in the past [14,15] but recent developments in rheological techniques and the availability of rigid particle data to use as a comparison make an additional study desirable.

Two media were selected for study: water and ethane diol; these were chosen mainly to study the effect of changing the medium viscosity but also because it was hoped that the different media would have different swelling characteristics and hence lead to different deformabilities. In the event, however it turned out that the equilibrium swelling characteristics of the starch in water and ethane diol were almost identical.

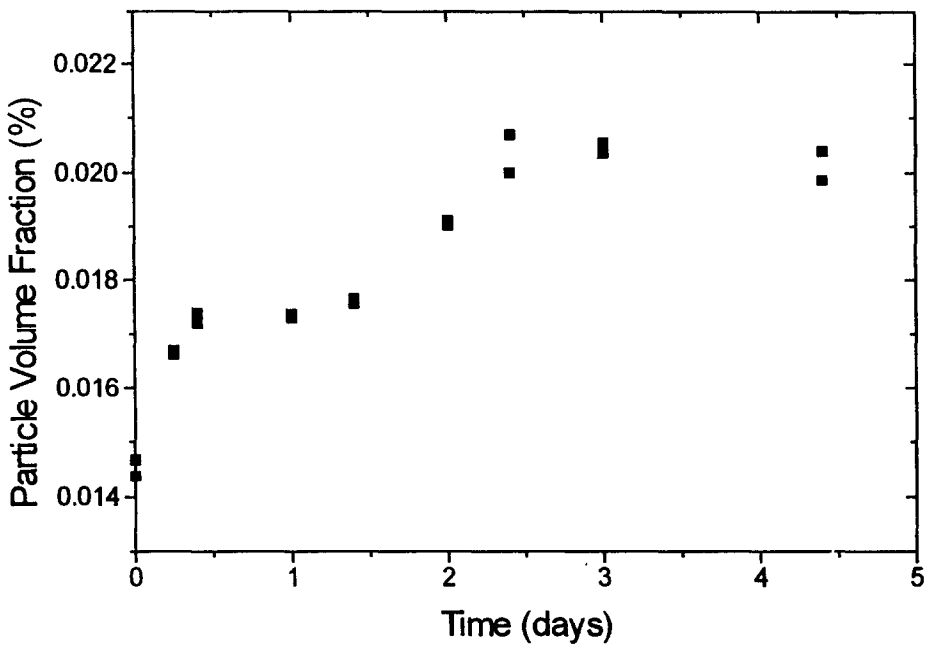

Fig. 5. Swelling of maize starch in ethylene glycol, measured using Mastersizer.

Samples in water were prepared by weighing out the appropriate amounts of water and starch into a container and mixing with a spatula. Rheological and light scattering studies indicate that swelling of the starch granules in water is almost immediate. This was not the case, however, for the starch suspensions in ethane diol. Because the starch contains a certain amount of moisture to start with it was necessary to dry the starch in a vacuum oven at 80°C, on this basis the starch was found to contain 11% w/w moisture, which is in agreement with the results of Lips [16]. When the dried starch is added to ethane diol swelling of the granules then takes place over a period of a few days.

This process can be followed using static small angle light scattering on the Malvern Mastersizer. A freshly made suspension was placed in the instrument and the volume concentration, determined from the obscuration [16], was monitored over a period of days. Results from this exercise are shown in Fig. 5, which demonstrates that equilibrium swelling is not achieved until some three days after the suspension's preparation. A similar exercise for corn starch in water demonstrates that the swelling is almost immediate.

These measurements give the degree of swelling of the cornstarch in water and in ethane diol to be in the region of 1.73 v/v with a probable

error of 0.08, in reasonable agreement with the results of Lips [16] and Evans [17]. The similar swelling of the starch in the two media can be confirmed to greater accuracy by measuring the sediment volumes formed by the suspensions. Measurements were carried out by weighing 10 g amounts of corn starch into two beakers, adding excess medium, mixing vigorously with a spatula, and allowing a sediment to form under gravity, after ensuring the granules were fully swollen. The supernatant was decanted off and the weight of sediment measured, this procedure gave the weight concentrations for the suspensions in water and ethane diol to be 0.5352 and 0.5083 respectively. The resulting values for the starch volume fraction were 0.416 ± 0.001 for both suspensions (assuming the partial specific volume of the starch to be 0.62), confirming that the swelling for starch in water and ethane diol is almost identical.

A further measure of the swelling ratio (Q) was obtained by measuring the intrinsic viscosity of dilute suspensions of starch in water, the intrinsic viscosity being given by

$$[\eta] = \frac{\eta_R - 1}{\phi} \tag{1}$$

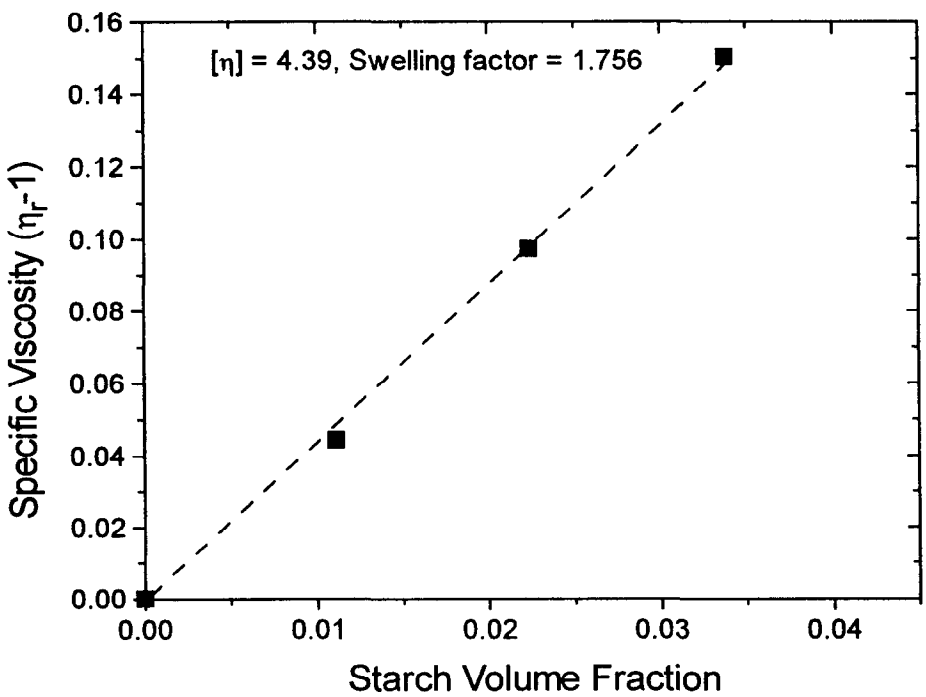

Fig. 6. Specific viscosity (η_{sp}) as a function of starch volume fraction (ϕ_s). Slope gives intrinsic viscosity [η].

In the above η_R is the relative viscosity of the suspension and ϕ is the volume fraction. For suspensions of rigid spherical particles Einstein [18] showed that [η] should equal 2.5, if we then use the volume fraction of the unswollen starch (ϕ_s) instead of ϕ then [η] will take on the value 2.5Q. Data for η_R were measured using a Contraves LS30 in a couette geometry, problems with sedimentation were avoided as much as possible by making the measurements within a few seconds of placing the suspension in the rheometer. Figure 6 shows the resulting data in the form of $\eta_R - 1$ as a function of ϕ_s for the maize starch, the slope of this plot gives [η] to be 4.39 the resulting value of Q is thus 1.756, in good agreement with the light scattering results. The results from the sedimentation studies and measurements of Q give the maximum packing fraction ($\phi_{max} = \phi_s \cdot Q$) of the starch granules to be 0.72 ± 0.04, whilst the value generally quoted for mono-sized spheres is 0.6–0.64.

Particle size of the starch was also measured using the Mastersizer, the results from which are shown in Fig. 7. The mean size (D(4,3)) is 15.9 μm and the width of the distribution is 0.87 of the mean.

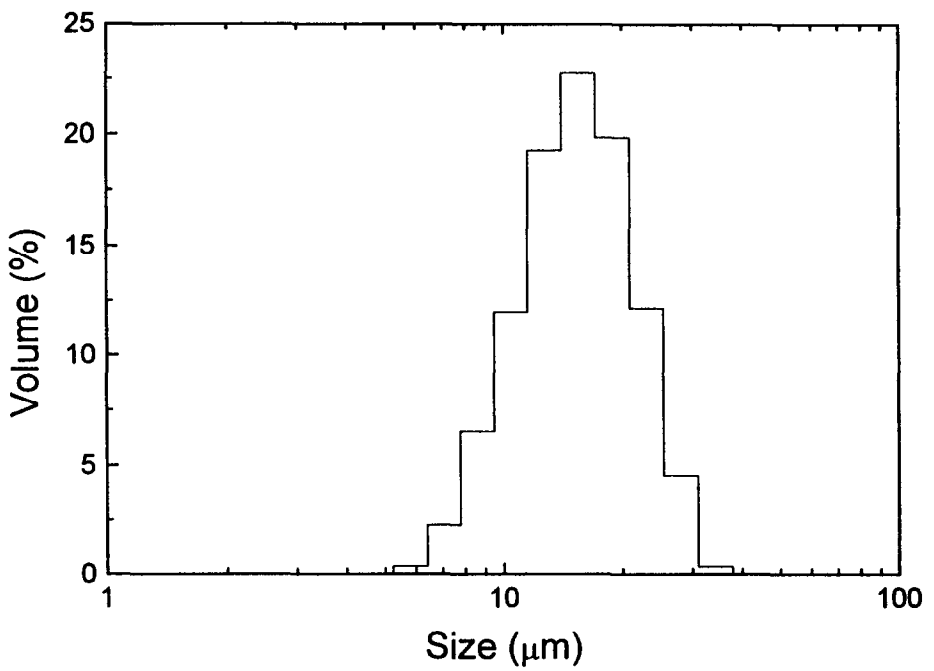

Fig. 7. Size distribution for maize starch from Mastersizer. Average diameters are: D(4,3) = 15.9, and D(6,3) = 17.6 (μm).

Rheological measurements

As has already been discussed in the introduction, the use of controlled stress rheometry is highly suited to the study of dilatancy and in this study the technique was used throughout. The instrument used was a Rheometrics RSR 8600 with either parallel plate or cone and plate geometries and water bath temperature control. Samples were covered with oil to prevent evaporation or, in the case of the glycol suspensions, to prevent uptake of water vapour. A number of problems, associated with the large size of the starch granules, were encountered in making the rheological measurements, these problems and the methods used to circumvent them are discussed in detail in this section.

(a) Sedimentation

The large size of the particles leads to a number of problems in making rheological measurements on the suspensions, the main one in this case being that of sedimentation. In the dilute state the Stokes' equation gives the sedimentation velocity of the starch granules to be

$$v_{sed} = \frac{2a^2 \Delta\rho G}{9\eta_m} \tag{2}$$

Here a is the radius of the particles, $\Delta\rho$ is the density difference, G is the acceleration due to gravity and η_m is the medium viscosity, the resulting v_{sed} is of the order of 2 mm/min. Whilst this would be expected to be less in the case of a concentrated suspension, sedimentation still poses severe problems to making accurate and reproducible rheological measurements.

A unique property of dilatant suspensions makes it possible to avoid the problem of sedimentation, and is related to the underlying mechanism of shear thickening. In truly dilatant materials, as first observed by Reynolds [1], the particles of the suspension, when shear thickening occurs, attempt to occupy a larger volume than the sum of the constituents of the suspension (particles and medium). A side effect of this behaviour is that the process of dilatancy will counteract sedimentation making it possible to derive rheological profiles that avoid the effects of sedimentation.

Two methodologies were employed in the measurements. In both cases, after the sample had been placed in the rheometer, a stress was applied above the dilatant transition so as to prevent sedimentation.

The stress/time profile then applied to the sample was similar to one of those illustrated in Fig. 8. In the first case (Fig. 8a) the sample is subjected to a stress that continuously decreases with time to zero over a period of 100 s followed by a subsequent increase back to the initial

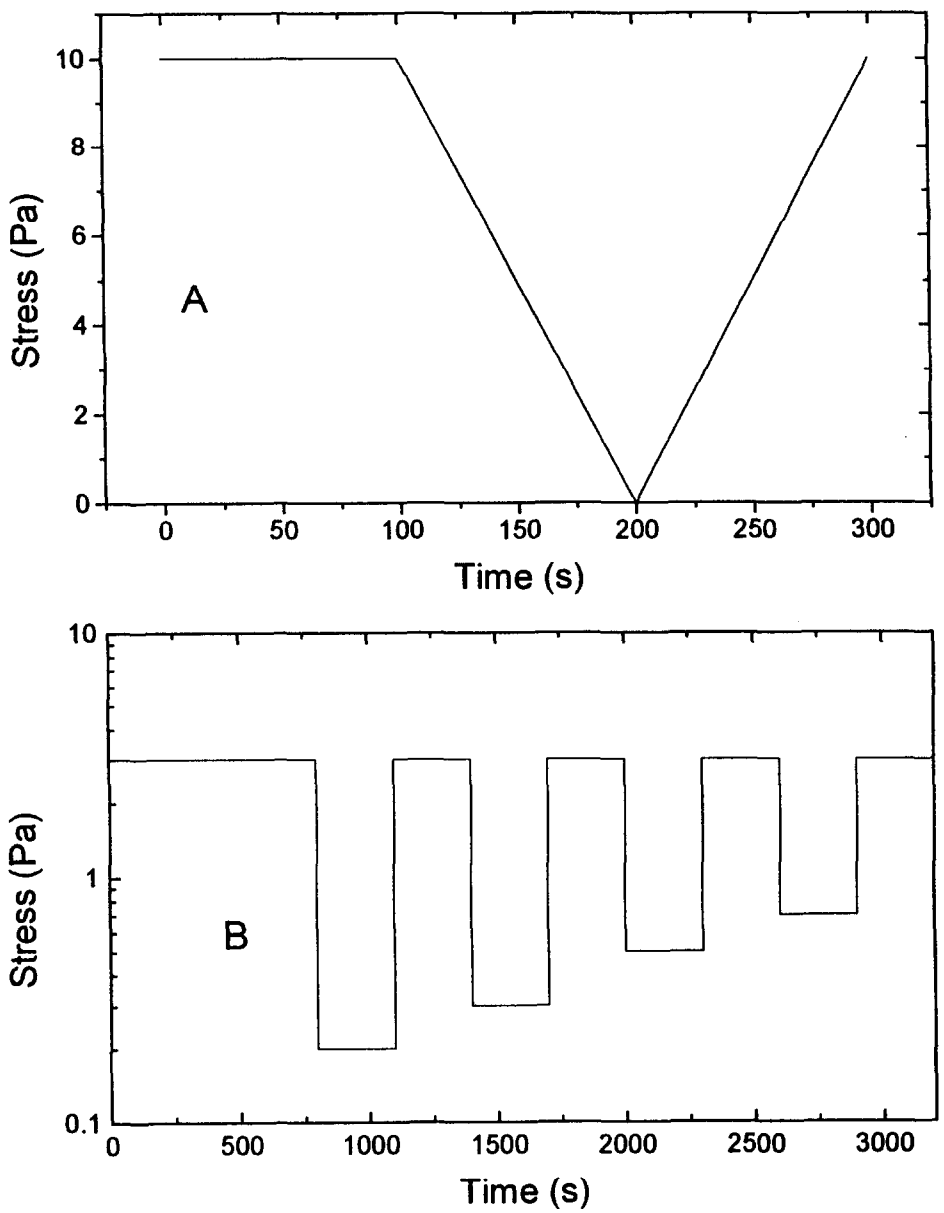

Fig. 8. Illustrations of stress histories applied to starch suspensions.

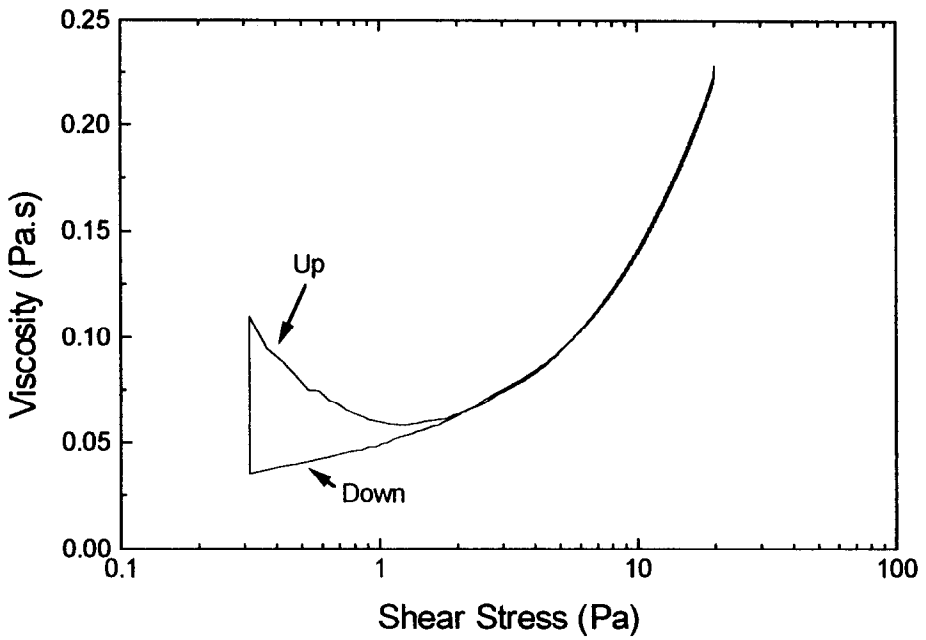

Fig. 9. Typical result obtained from stress history illustrated in Fig. 6a.

value over the same period. A typical result from this type of measurement is illustrated in Fig. 9. Whilst this method is very rapid and provides reasonable results near and above the dilatant transition, at stresses well below the transitions the results are dominated by inertial effects on the rotor of the instrument, making accurate measurements at these stresses impossible.

The other methodology employed is illustrated in Fig. 8b. Here, after conditioning at a stress above the dilatant transition the stress is stepped to the value at which the measurement is to be made. After the step in stress the viscosity is monitored as a function of time for a period of ~100 s during which period the viscosity falls due to the effects of the sedimentation, a typical response is illustrated in Fig. 10. The viscosity of the suspension is taken as being that measured immediately after the stress changes from the conditioning value. This technique allowed measurements to be made at stresses as low as 0.1 Pa.

Both of these techniques suffer from one major disadvantage, which is that it is impossible to use them to study time dependent effects, such as thixotropy. However, the lack of strong shear thinning and the ready sedimentation observed in these suspensions does argue that aggrega-

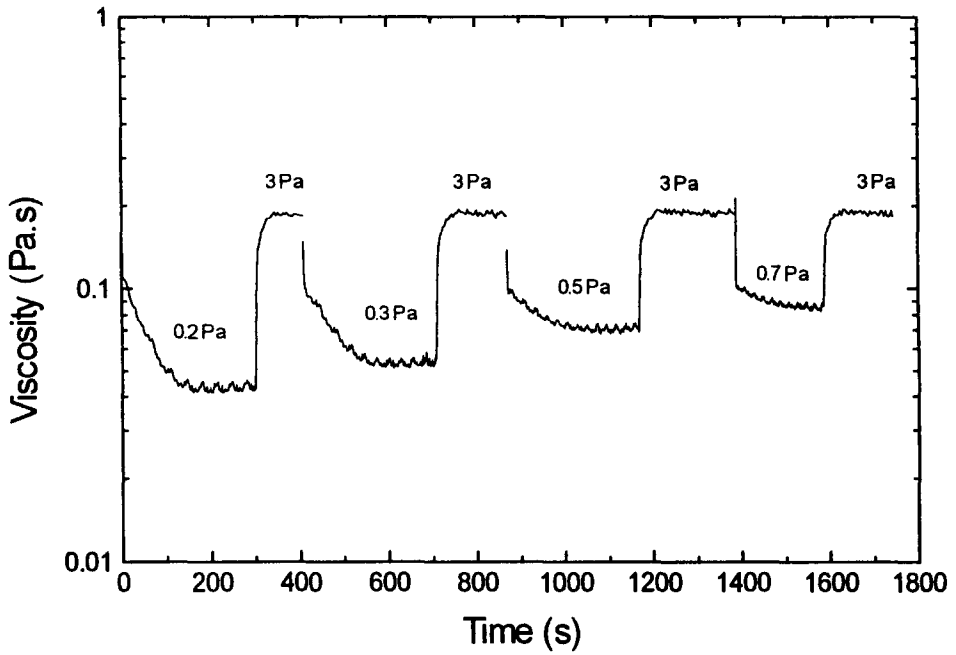

Fig. 10. Typical result from stress history illustrated in Fig. 6b.

tion does not play a role in the rheology, as a result time dependent effects should be largely absent.

(b) Wall slip

This is a phenomenon encountered in a wide variety of materials and is, in solutions and suspensions at least, associated with a depletion of material near the rheometer surfaces. The increased shear in this region leads to erroneously low values of the viscosity being measured. A number of authors have studied the phenomenon [19,20] and have considered methods for removing or correcting for the error. Two methods are generally applied, one is to roughen the surfaces of the plates in the rheometer in order to prevent slip. The other method involves making measurements with different gaps between the plates or angles between the cone and plate and extrapolating to large gaps/angles, the assumption being that the slip layer does not change with gap [19].

The possibility of slip in the starch suspensions was investigated by making measurements using parallel plate geometries, with and without roughened surfaces. Roughness was achieved in this case by gluing disks of emery paper onto the plates, results for the two cases are shown

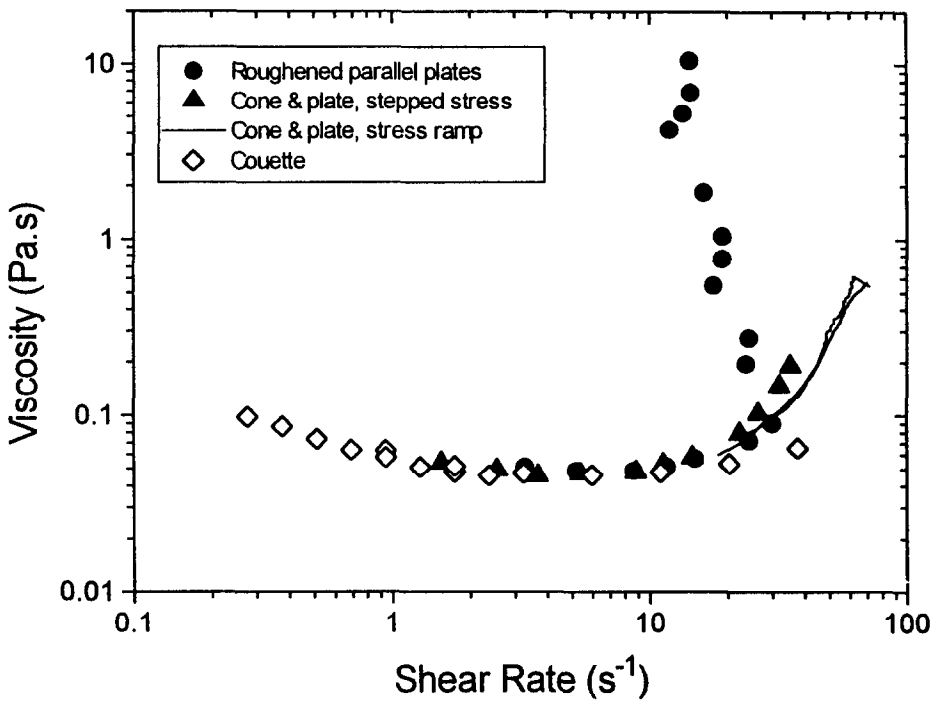

Fig. 11. Effect of wall slip on dilatant response.

in Fig. 11. It is evident that the two surfaces do give different results, however this is only the case above the dilatant transition, below it no slip seems to occur. The nature of the response above the transition can be dramatically different depending on whether slip is occurring. If slip does occur then the viscosity rises gradually, rather than suddenly as for the no-slip situation. Also, the response as a function of time differs for the two cases. Whilst a constant value of the shear rate is obtained for the smooth plates, the roughened plates produce a shear rate which fluctuates randomly with time. This phenomenon is observed in other dilatant suspensions [3,13] though no explanation for it is available it is undoubtedly related to the fluctuations in the suspension microstructure occurring during flow.

(c) Particle migration

A well documented phenomenon occurring in suspensions of large particles in inhomogeneous flows such as parallel plate rotational flow and pipe flow is the tendency for the particles to migrate to regions of low shear rate. If this behaviour occurs then use of such geometries for

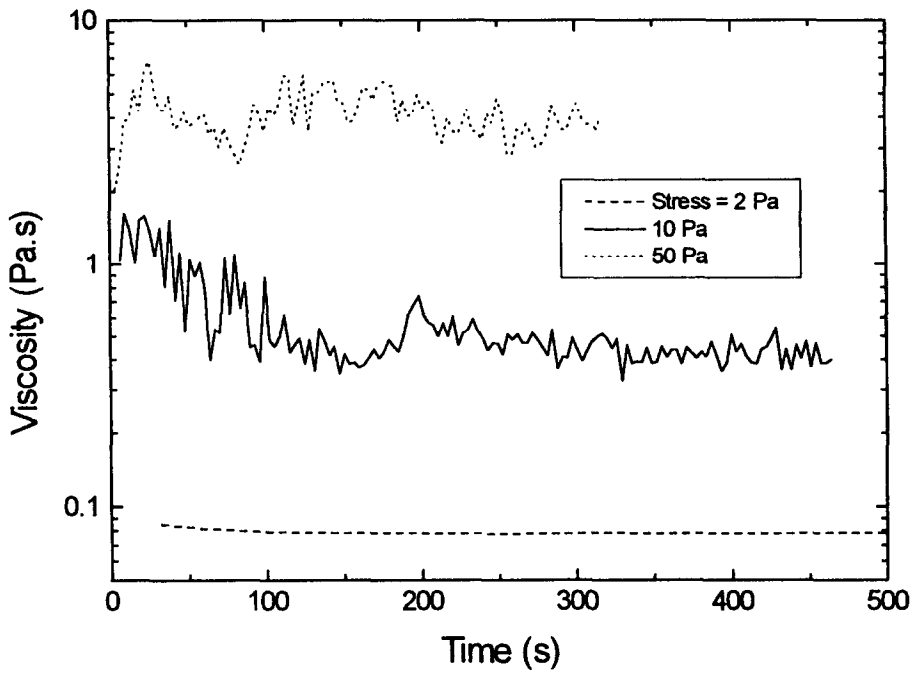

Fig. 12. Viscosity as a function of time for parallel plates.

the measurement of rheological properties is unwise. In parallel plate flow as used in the above studies migration is to be suspected if the viscosity response shows a decrease with time during the application of a steady shear stress. Figure 12 shows that such behaviour is exhibited by the starch suspensions making undesirable the use of parallel plates to measure these systems.

Unfortunately the method used to counteract slip in the parallel plate geometry cannot be used with cone and plate making it necessary to choose between slip effect or particle migration in these measurements. Since the parameter of interest here is the critical shear rate for the onset of dilatancy which is not significantly affected by the wall slip observed it was decided to make measurement using cone and plate.

Results and discussion

Figures 13a and b show results for the viscosity as a function of shear rate in water and ethane diol. The two sets of data show that the response of the suspensions in different media are very similar, indicat-

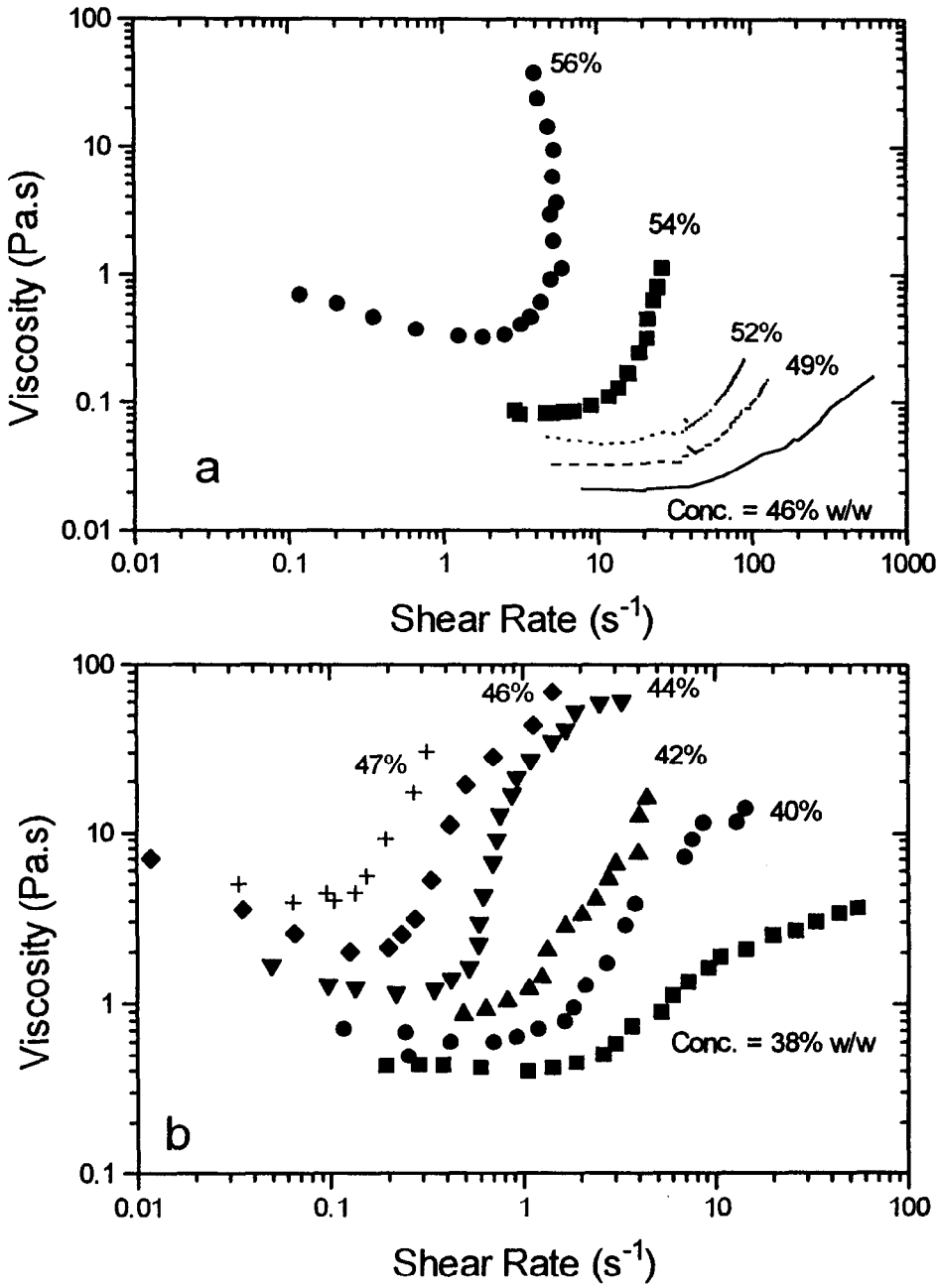

Fig. 13. Viscosity shear-rate data for waxy maize starch suspensions in water (a) and ethane diol (b).

ing that the state of dispersion of the starch in both cases is also comparable. A feature of these results, common to systems exhibiting dilatancy is the increasingly abrupt rise in viscosity as the concentration is increased, though in reality the viscosity is likely to rise still more steeply if the effects of wall slip are taken into account. In addition, the shear-rate for the onset of dilatant flow decreases as the concentration increases.

In order to compare results from different media and the effects of particle deformability on the rheology of starch suspensions it is best to consider the effects of concentration on parameters that characterise the curves in Figs. 13a and b. Two parameters are employed here, the high shear plateau viscosity (η_∞) and the critical shear rate for dilatancy ($\dot{\gamma}_c$). The first of these is simply the minimum viscosity displayed by the suspension as a function of shear rate, as illustrated in Fig. 14, whilst the latter is found from the intersection with η_∞ of a line extrapolated

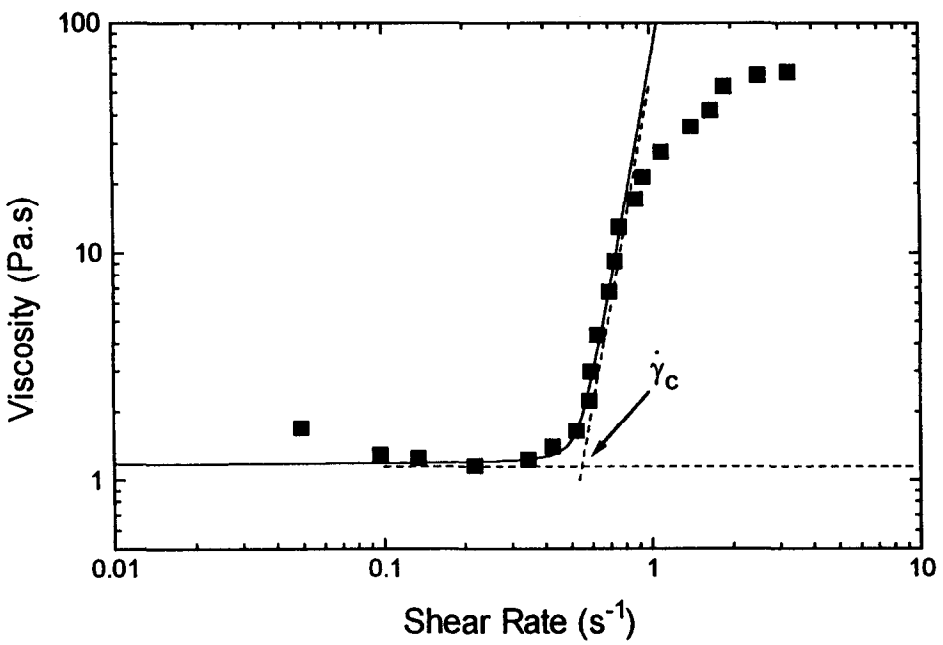

Fig. 14. Illustration of determination of critical shear-rate, solid curve shows fit of Eq. (3) to data (not all data were included in fitting process).

from the steepest portion of the viscosity shear rate curve. In fact $\dot{\gamma}_c$ was determined by fitting a hyperbolic function to the data using a Levenberg–Marquardt non-linear least squares algorithm i.e.

$$\log(\eta) = b\cdot\sqrt{\log\left(\frac{\dot{\gamma}}{\dot{\gamma}_c}\right)^2} + a + b\cdot\log\left(\frac{\dot{\gamma}}{\dot{\gamma}_c}\right) + \log(\eta_\infty) \tag{3}$$

where 2·b is the slope of the dilatant portion of the curve and a is the degree of curvature at the dilatant point. No significance should be attached to the form of this equation, it is simply used here as a convenient means of calculating $\dot{\gamma}_c$.

High shear limiting viscosity

Values for $\eta_{r\infty}$ (= η_∞/η_m) as a function of the particle volume fraction (ϕ_p) are shown in Fig. 15, agreement between the results for water and ethane diol is excellent, which indicates that the starch is dispersed to the same extent in both cases. These data can be compared with any of

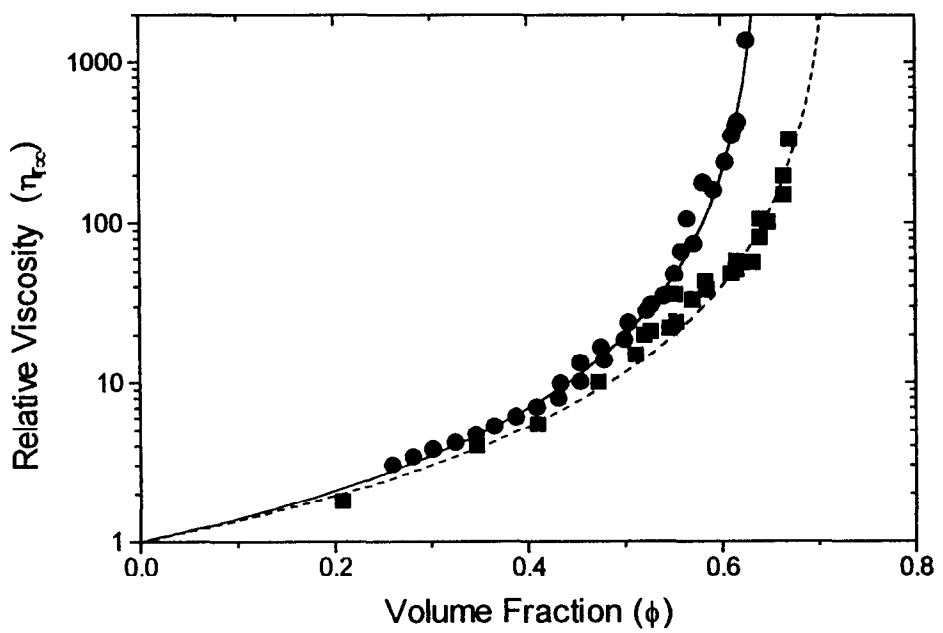

Fig. 15. Viscosity concentration data for starch (squares) and hard spheres (circles). Also shown are fits of Eq. (4) to data.

a number of semi-empirical relationships for $\eta_{r\infty}(\phi)$, that due to Krieger [21] is employed here:

$$\eta_{r\infty} = \left(1 - \frac{\phi_p}{\phi_{max}}\right)^{-\phi_{max}(\eta)} \tag{4}$$

where ϕ_{max} is the maximum packing fraction and $[\eta]$ is the intrinsic viscosity. The best fit of Eq. (4) to the data gives $[\eta] = 2.88$ and $\phi_{max} = 0.722$, the latter being in excellent agreement with the sedimentation result. $[\eta]$ is rather high compared to the theoretical value of 2.5 for spheres, however, a similar fit to hard sphere data [22,23], also shown in Fig. 15 gives $[\eta] = 3.18$ in reasonable agreement with the starch data. The value of $\phi_{max} = 0.647$ is within the expected range for this type of data.

However, the value of ϕ_{max} obtained from the starch data is rather high compared to that found for model hard-sphere systems (0.6–0.64). There are a number of factors which may account for this: particle size distribution or shape may affect the packing of the particles, particle deformability may play a role in the suspension rheology, or the measured swelling ratio (Q) of the particles may be incorrect.

A number of workers have studied the effect of particle size distribution on the values of ϕ_{max} obtained [24–26]. Generally it has been found that bimodal or multimodal distributions produce the densest packings. Since bimodal distributions with an extreme size ratio will only produce a ϕ_{max} of around 0.7–0.74, it seems unlikely that the size distribution observed for the starch would give a ϕ_{max} of this order.

In order to consider whether or not the particle deformability has a significant effect on ϕ_{max}, we need a relationship between this property, the stresses experienced by the particles during the experiments and their rheology. Recent work by Buscall [27–29] has considered the similar situation of suspensions of particles with long range forces between them. It was proposed that the rheology of suspensions of particles with such interactions could be modelled on the basis of an effective hard sphere. The principle of the model is to calculate an effective radius (a_{eff}) for the particles using the Barker and Henderson [30] equation, modified to include a granular temperature:

$$a_{eff} = \frac{1}{2}\int_0^\infty \left\{1 - \exp\left[\frac{-U(r)}{\left(kT + \frac{\tau(a_0/2)^3}{K}\right)}\right]\right\} dr \tag{5}$$

Here U(r) is the interparticle pair potential, r the centre–centre particle separation, τ is the shear stress, a_0 the particle radius assumed in calculating ϕ, the measured volume fraction, k and T is the Boltzman constant and absolute temperature, and K is a constant of order 1. The effective particle radius can now be used to calculate an effective volume fraction of the particle:

$$\phi_{eff}(\tau) = \phi \left(\frac{a_{eff}}{a_0} \right)^3 \tag{6}$$

which now allows the viscosity to be calculated, in this case using the Krieger–Dougherty equation [21].

$$\eta_r(\tau) = \left(1 - \frac{\phi_{eff}}{\phi_{max}} \right)^{-[\eta]\phi_{max}} \tag{7}$$

In the case of the starch granules we introduce an interparticle potential (U(r)) based on the Hertz model [31] for the force between two elastic spheres.

$$U(r) = \frac{32}{15} a_0^{\frac{1}{2}} \left(a_0 - \frac{r}{2} \right)^{\frac{5}{2}} \left[\frac{G_p}{(1-\sigma)} \right] \tag{8}$$

Assuming $[\eta]$ = 3.18 and ϕ_{max} =0.647, as obtained from the hard sphere data then it is possible to make predictions of the relative viscosity as a function of the volume fraction for different particle moduli. As the predicted viscosity is dependent on stress, a value has to be selected for this parameter, 1 Pa was used as the viscosity at this stress was close to $\eta_{r\infty}$ for the starch suspensions. Predicted values of $\eta_{r\infty}$ are compared with the results found for starch suspensions in Fig. 16 from which it is evident that, in order to account for the high value of ϕ_{max} the particle modulus must be ~10^4 Pa. This value seems unreasonably low, bearing in mind the degree of swelling of the starch granules, unless it is assumed that the granule is inhomogeneously swollen and has a highly deformable outer layer.

The only remaining explanation for the high value of ϕ_{max} is that the estimated volume concentrations are incorrect. There are two major possible sources of error; both giving rise to incorrect values of Q. One possibility is that the non-spherical nature of the starch granules is

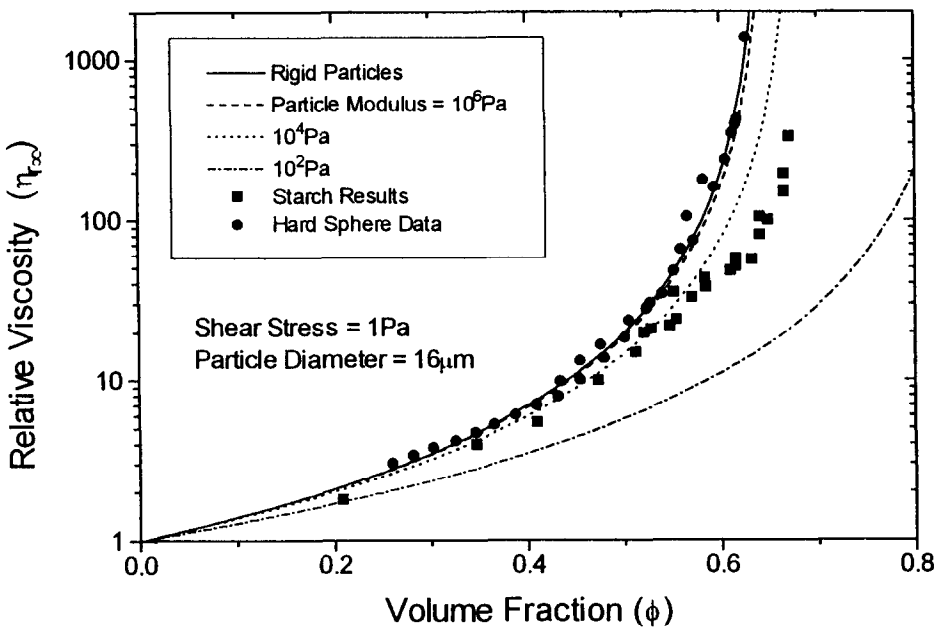

Fig. 16. Comparison of measured viscosities with predictions for deformable particle suspensions (from Eqs. (5)–(8)).

leading to overestimates of the volume concentration. This is certainly possible in the case of the measurements of [η], Jefferey [32] and Simha [33] have shown that even particles with moderate aspect ratios (<2) can have values of [η] significantly higher than 2.5, this would lead to an overestimate of the swelling factor Q. Similar errors are also possible in the light scattering measurements. It is also possible that the particle specific volumes assumed for the components are incorrect. The value of 0.62 for starch has a basis in measurement [16], but the same is not true for the media, where the densities of the pure materials were used.

It is difficult to draw any firm conclusions from the above discussion. It may be that the particles are showing the effects of size and shape polydispersity, or there may well be errors in the assumptions used to calculate the volume fraction. However particle deformability does not seem to be playing a significant role.

Dilatant behaviour

Dilatant shear rates, measured as described above using Eq. (3), are shown as a function of concentration in Fig. 17a. There is a strong

dependence of $\dot{\gamma}_c$ on concentration and on medium viscosity, if we consider the critical shear stress for dilatancy (σ_c) which is simply the product $\dot{\gamma}_c\eta_\infty$ as shown in Fig. 17b we see that there is much weaker dependence on concentration.

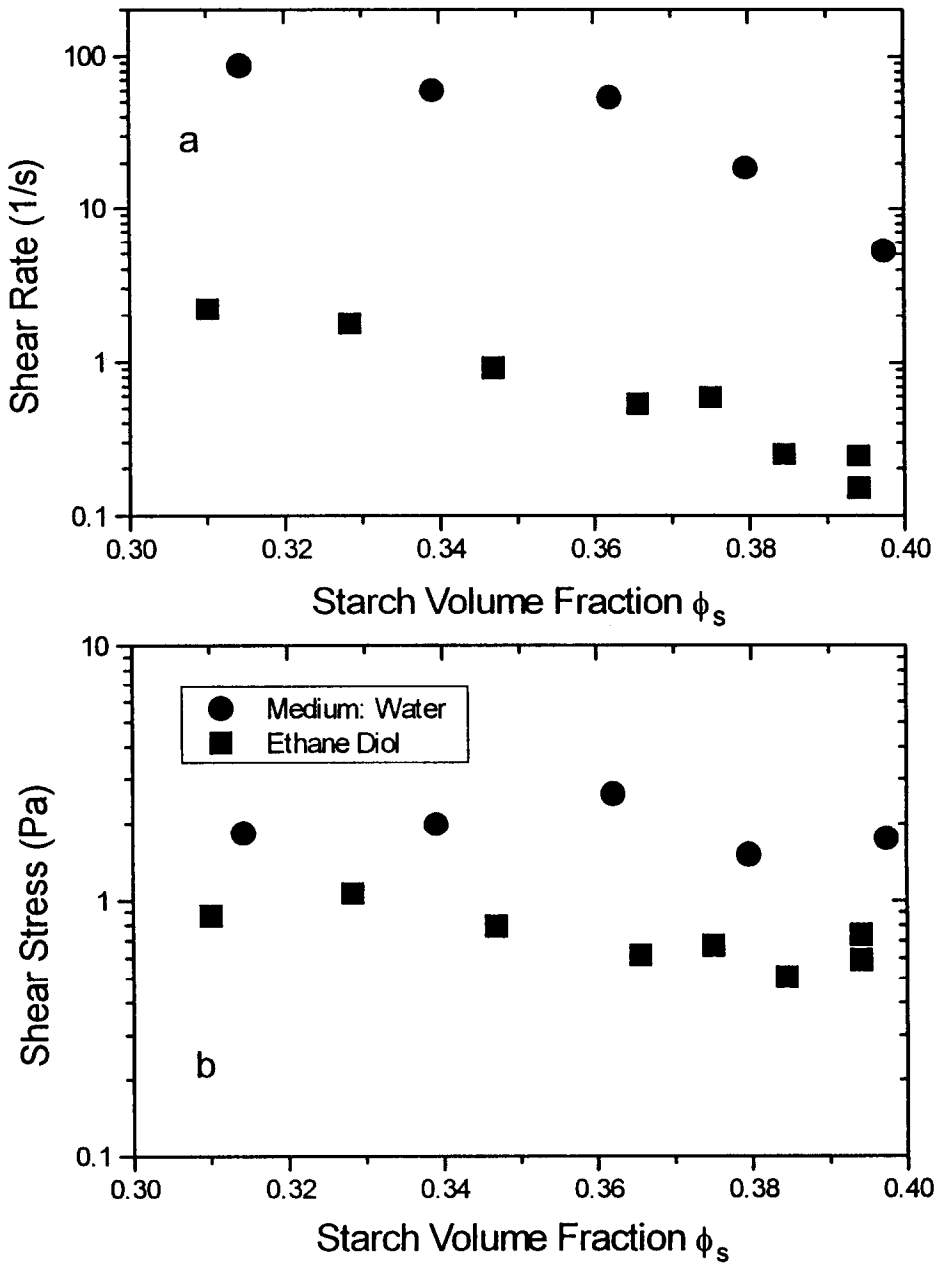

Fig. 17. Effect of starch volume fraction on critical shear-rates (a) and shear stresses (b).

As with the relative viscosity it would be desirable to plot these results in the form of some scaling variable. It is known that the medium viscosity and particle size will affect the dilatant transition, but the exact nature of this effect is unclear, especially in the case of the particle size, thus it is unclear exactly what scaling variable would be appropriate for dilatancy. Two forms have been proposed in the literature [2,5], the Peclet number

$$Pe = \frac{\dot{\gamma}_c \eta_m a^3}{kT} \tag{9}$$

and an a^2 scaling

$$\dot{\gamma}_c \eta_m a^2 \tag{10}$$

The above two scaling relations reflect different approaches to the underlying mechanism of dilatancy, Eq. (9), reflects the idea [5] that the transition has its origins in or is related to the Brownian motion of the particles. Equation (10), on the other hand reflects the proposal [2,8] that hydrodynamic forces on the particles are the dominant factor in controlling the dilatant transition.

Both Eqs. (9) and (10) are based on the assumption of uniform rigid spherical particles and no attempt is made to take into account phenomena such as particle deformability or long range interactions. It is expected that both these phenomena will have a significant effect upon the dilatant behaviour though the exact nature of the effect is unclear, comparison of the results obtained from deformable particles with that from model hard sphere suspensions should clarify the nature of the effect of particle deformability.

However, since there is no clear consensus as to the correct scaling variable to use it is necessary to compare the starch data with hard sphere results using both Eqs. (9) and (10). Because of the strong dependence of γ_c on the concentration, uncertainties in ϕ, arising from doubts about the degree of swelling discussed above, could have a significant effect on the comparison of different sets of data. In order to make these comparisons a more accurate measure of the concentration is required. Whilst such a direct measure of the concentration is not available, a useful compromise is to make use of $\eta_{r\infty}$. It has already been established that in principle there is a unique relationship between this parameter and ϕ which is given by Eq. (7), we may thus use $\eta_{r\infty}$ instead

of ϕ. The results of doing this are shown in Figs. 18a and 18b for Eqs. (9) and (10) respectively.

Also shown in Figs. 18a and b are values for $\dot{\gamma}_c$ obtained for a model hard sphere system consisting of mono-sized PMMA particles [34]. Data for two particle sizes are shown, 817 nm and 390 nm. It is worth noting at this point that the Peclet number scaling does appear to work better for the hard sphere data presented here, though it is probably unreasonable to expect such a scaling to work for particles with sizes similar to the starch, where Brownian forces are very weak. Indeed Fig. 18a confirms that there is a large discrepancy between the starch data and that of the model system, as might be expected for the Peclet number scaling. However, Fig. 18b shows that a similar result is found for the a^2 scaling, there being almost two orders of magnitude between the two sets of data. The scaling used in this figure, based as it is on hydrodynamic considerations [2,8], might be expected to work for the larger particle sizes. The fact that it does not, would imply that the particles are behaving in a deformable manner at stresses above the dilatant point, even though the evidence for such behaviour at stresses below $\dot{\gamma}_c$ seems to indicate otherwise.

Other possibilities remain however; it may be that, since there is a distribution of particle sizes, the average diameter being used for scaling $\dot{\gamma}_c$ is not appropriate. Comparisons of number and weight average particle diameters ($\langle M_W \rangle / \langle M_N \rangle = 1.11$), obtained from Fig. 7 indicate that the maximum error in scaling ($\langle M_W \rangle^3 / \langle M_N \rangle^3 - 1$) is in the region of 36% which does not account for the difference between the two sets of data. However the Mastersizer is rather insensitive to the presence of small particles in a distribution and it was felt that a further test was appropriate.

A sample of maize starch was fractionated to remove particles with diameters below ~10 μm by repeatedly centrifuging and redispersing the sediment at a rate calculated to allow all the particles above ~10 μm to form a sediment. Both the supernatant and the sediment were kept and analyzed using the Mastersizer, the results from which are shown in Fig. 19. The concentration of the sediment was measured by drying overnight in a vacuum oven at 80°C and adjusted to 52% w/w. The flowcurves for the sediment and for the unfractionated starch are shown in Fig. 20a.

This figure shows that whilst the high shear limiting viscosity for the two suspensions is almost identical, there is a difference in the dilatant transition. Whilst this is not large and would certainly not account for

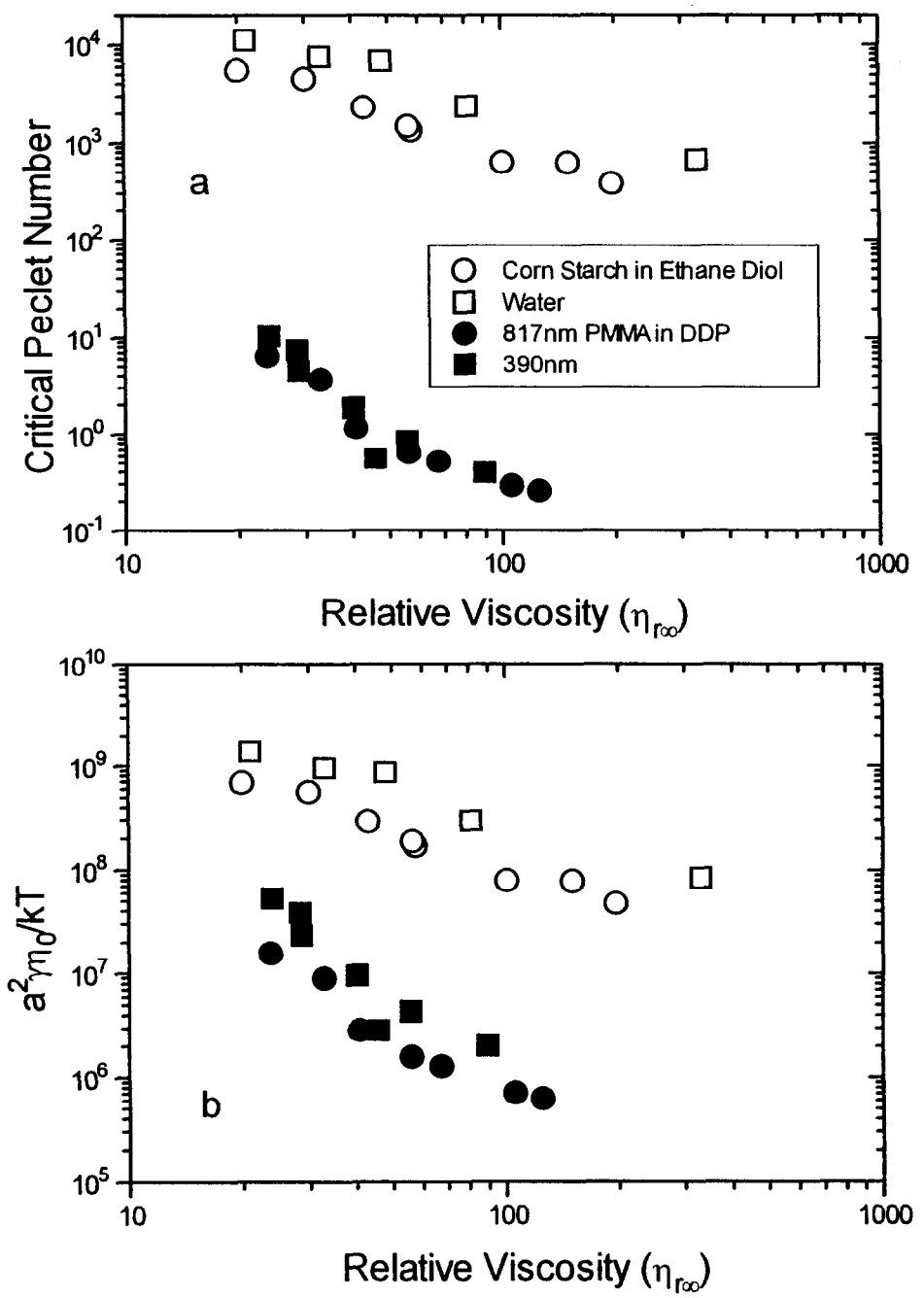

Fig. 18. Comparison of critical shear-rates for starch and hard sphere data; (a) scaled using Eq. (9) and (b) using Eq. (10).

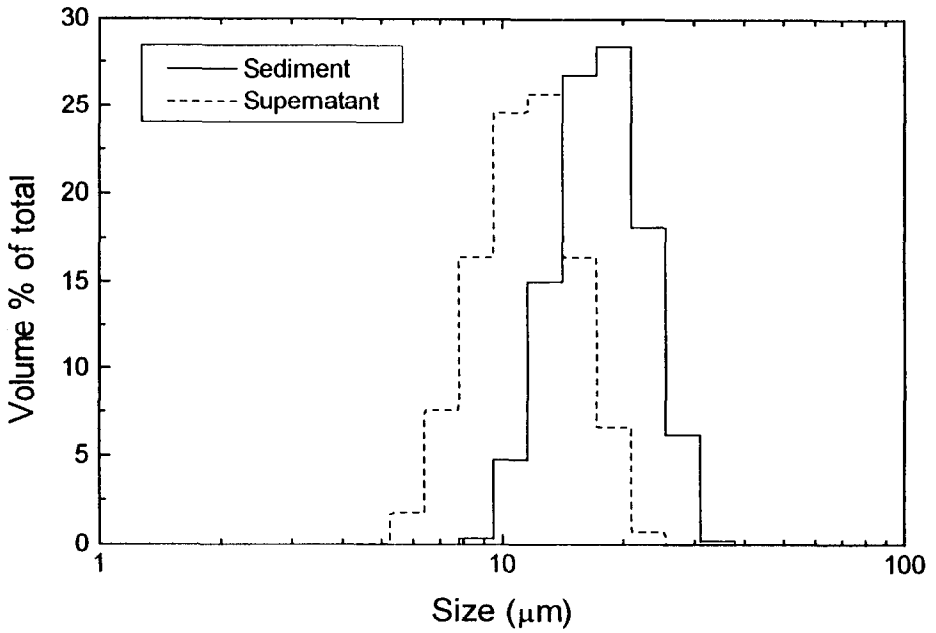

Fig. 19. Size distributions of fractionated starch as measured on the Mastersizer.

the difference between the starch and the hard sphere data, it may be that it can be accounted for by the difference in diameters between the two samples, the fractionated sample being the larger. Figure 20b shows the result of plotting the Peclet scaling on the X-axis assuming a diameter of 19.1 μm for the fractionated and 17.6 μm for the unfractionated suspension, agreement between the two suspensions improved over that for Fig. 20a, the remaining discrepancy may be a result of the narrower size distribution for the fractionated sample.

It would seem from the above discussion that there is a significant difference between the starch and hard sphere data that can only be accounted for by the deformability of the starch granules. This conclusion appears to be at odds with that drawn from the high shear limiting viscosity ($\eta_{r\infty}$) data in that it is not clear that this parameter is affected by particle deformability. Whilst it might seem difficult, at first sight, to reconcile the two particle behaviours, below and above $\dot{\gamma}_c$ it is possible that particles undergoing dilatant flow may experience considerably different stresses to those undergoing normal flow, even though the bulk stresses experienced by the suspension may not be all that different. The reason behind this lies in the supposition that lubrication forces between particles break down during dilatancy [11].

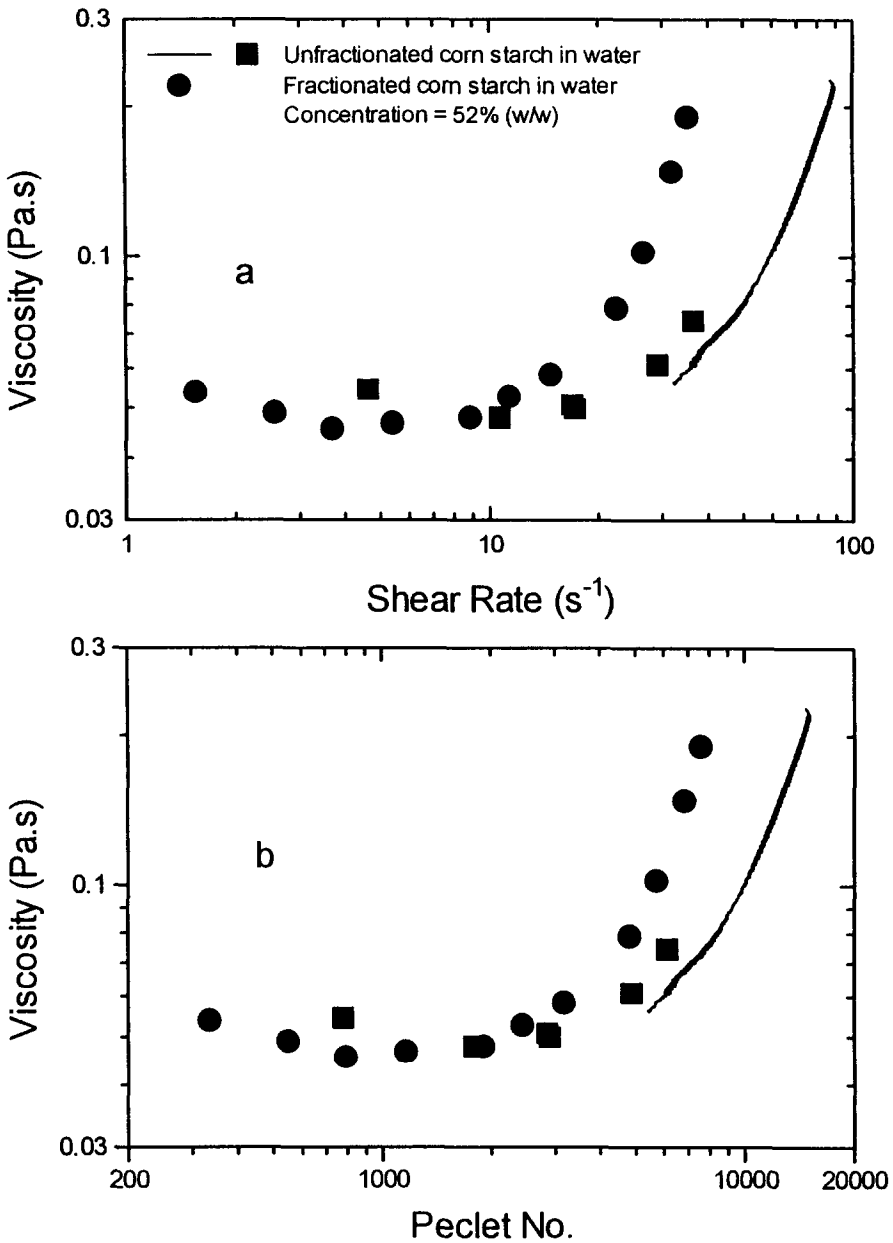

Fig. 20. Comparison of fractionated and unfractionated starch suspensions as a function of shear-rate (a) and Peclet No. (b).

In suspensions undergoing normal flow it is believed that the forces between particles are mediated entirely by the viscous medium in which they are suspended. It is, however likely that this is not the case in suspensions undergoing dilatant flow. Experimental evidence exists [1], for an apparent volumetric dilatancy, where the particles in the suspension attempt to occupy a volume greater than the sum of the particle volumes and the volume of the suspending medium. This indicates that the particles are forming what is essentially a close packed structure. Particle forces, in such a scenario, would no longer be mediated by the medium but would involve direct mechanical contacts more akin to those present in powder systems.

Structures of this nature are known to have highly inhomogeneous distributions of contact forces [35,36], one consequence of which is that relatively few particles in the structure will bear the majority of the load applied to the overall suspension at any one time. Thus the maximum stresses experienced by individual particles will undergo a significant increase during the transition from normal to dilatant flow, even though the overall stress applied to the suspension may not increase significantly. This would explain the observation that whilst the starch appears to behave in a similar fashion to the model hard sphere suspension during normal flow, since the particles are not significantly deformed, the dilatant behaviour of the starch is quite different, and particle deformability plays a dominant role.

References

[1] O. Reynolds, Phil. Mag., 20 (5) (1885) 469.
[2] R.L. Hoffman, Trans. Soc. Rheol., 16 (1) (1972) 155.
[3] H.M. Laun, R. Bung, S. Hess, W. Loose, O. Hess, K. Hahn, E. Hadicke, R. Hingmann, F. Schmidt and P. Lindner, J. Rheol. 36 (4), (1992).
[4] R.L. Hoffman, J. Colloid Interface Sci., 46 (3) (1974) 491.
[5] G.N.M. Choi, Thesis, Ann Arbor, MI, 1983.
[6] A.B. Metzner and M. Whitlock, Trans. Soc. Rheol., 11 (1958) 239.
[7] H.A. Barnes, J. Rheol., 33 (2) (1989) 329–366.
[8] W.H. Boersma, P.J.M. Baets, J. Laven and H.N. Stein, J. Rheol., 35 (6) (1991) 1093.
[9] W.H. Boersma, J. Laven and H.N. Stein, AIChE J., 36 (3) (1990) 321.
[10] S.J. Willey, J. Rheol., 26 (6) (1982) 557–564.
[11] Melrose and Ball, Private communication.
[12] G. Marrucci and M.M. Denn, Rheol. Acta, 24 (3) (1985) 317–320.
[13] P. D'Haene, J. Mewis and G.G. Fuller, J. Colloid Interface Sci., 156 (1993) 350–358.

[14] R.L. Hoffman, Adv. Colloid Interface Sci., 17 (1982) 161–184.
[15] A. Eastwood and H.A. Barnes, Rheol. Acta, 14 (1975) 795–800.
[16] A. Lips, P.M. Hart, I.D. Evans and M. Debet, in: G.O. Phillips, P.A. Williams and D.J. Wedlock (Eds.), Gums and Stabilisers for the Food Industry 6. Oxford University Press, 1992, pp. 335.
[17] I.D. Evans and D.R. Haisman, Starke, 7 (1982) 224.
[18] A. Einstein, Ann. Physik., 19 (1906) 289.
[19] H.A. Barnes, J. Non-Newtonian Fluid Mech. (1995).
[20] L. Vargas, J. Perez-Gonzalez and J.J. Romero-Barenque, J. Rheol., 37 (5) (1993) 867.
[21] I.M. Krieger, Adv. Colloid Interface Sci., 3 (1972) 111.
[22] J. Mewis and P. D'Haene, Makromol. Chem., Macromol. Symp., 68 (1993) 213–225.
[23] W.J. Frith, J. Mewis and T.A. Strivens, Powder Technol., 51 (1987) 27.
[24] R.F. Probstein, M.Z. Sengun and T-C. Tseng, J. Rheol., 38 (4) (1994) 811.
[25] R.J. Farris, Trans. Soc. Rheol., 12 (1968) 281–301.
[26] R.L. Hoffman, J. Rheol., 36 (1992) 947–965.
[27] R. Buscall, J. Chem. Soc. Faraday Trans., 87 (9) (1991) 1365–1370.
[28] R. Buscall, Langmuir, 8 (1992) 2077–2079.
[29] R. Buscall, Colloids Surfaces A, 83 (1994) 33–42.
[30] J.A. Barker and D. Henderson, J. Chem. Phys., 47 (1967) 2856; 4714.
[31] H. Hertz, Gesammelte Werke, Leipzig, 1895.
[32] G.B. Jeffery, Proc. Roy. Soc., A102 (1923) 163.
[33] R. Simha, J. Phys. Chem., 44 (1940) 25–34.
[34] Manuscript in preparation
[35] C. Thornton and D.J. Barnes, Acta Mechanica, 64 (1986) 45–61.
[36] P.A. Cundall and O.D.L. Strack, Geotechnique, 29 (1979) 47–65.